Special Feature: Nanostructured Materials

Research Report

Novel Photocatalysts Based on Periodic Mesoporous Organosilica

Takao Tani, Hiroyuki Takeda, Masataka Ohashi and Shinji Inagaki

Report received on June 29, 2011

ABSTRACT We constructed two types of novel photocatalysts utilizing light harvesting or photo-induced electron donating properties of biphenyl-bridged periodic mesoporous organosilica (Bp-PMO). For the light harvesting photocatalysis system, rhenium (Re) complexes were fixed in the mesochannels of Bp-PMO. Light energy absorbed effectively by the Bp groups in Bp-PMO was funneled into the Re complex in the mesochannels and sensitized photocatalytic CO evolution from CO_2 on the Re complex by a factor of 4.4 compared with direct excitation of the Re complex due to the light-harvesting of the PMO antenna. The PMO antenna also showed photoprotection effect on the CO-ligand dissociation from the Re complex by UV-light irradiation. For the donor-acceptor photocatalysis system, viologen (Vio) was attached onto the pore walls of Bp-PMO, which resulted in the formation of charge transfer (CT) complexes between the attached Vio and Bp in the framework. Excitation of the CT band was confirmed to induce electron transfer from Bp to Vio to promote persistent charge separation. Hydrogen was successfully evolved photocatalytically utilizing this charge separation mechanism for platinum loaded Vio-Bp-PMO. These findings demonstrated the potential of PMO for construction of a broad spectrum of photocatalysts by appropriate combination of the organic groups in the framework (light collecting part) and catalysts (energy or electron accepting part).

KEYWORDS Periodic Mesoporous Organosilica, Photocatalyst, Light Harvesting System, Electron Donor-acceptor System, Reduction of Carbon Dioxide, Hydrogen Evolution

1. Introduction

Periodic mesoporous organosilicas (PMOs), synthesized from 100% or less organic-bridged alkoxysilane precursors (R-[Si(OR')$_3$]$_n$: n≥2),[1] are a new class of functional materials having organic-inorganic hybrid frameworks and well-defined mesochannels (**Fig. 1**).[2] A broad spectrum of functionalities can be introduced into their frameworks by proper design of organosilane precursors with specific bridging organic groups (R).[3] In addition, some PMOs bearing interactive organic groups have been found to show molecular-scale lamellar periodicity of the organic groups in the framework.[4] From these unique features, PMOs have been attracting much attention for their potential use in various applications such as catalysts, adsorbent and sensors.

On the other hand, we recently found unique optical functionalities of biphenyl (Bp)-PMO such as strong light absorption,[5] efficient fluorescence emission[5] and light harvesting.[6] The light harvesting antenna property indicates the funneling of light energy absorbed by the Bp groups in the framework into a small amount of dyes placed in the mesochannels by Förster resonance energy transfer (FRET).[6] These key

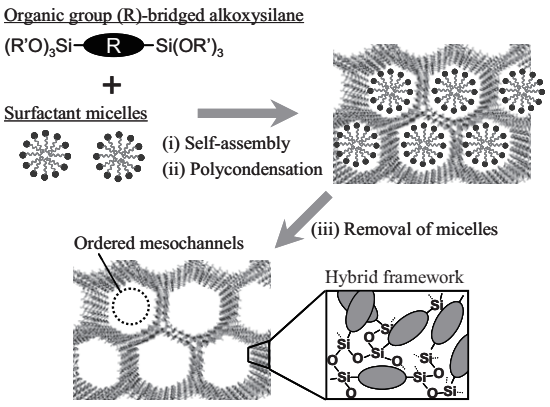

Fig. 1 A schematic image of preparation of PMO.

findings opened the potential of PMOs for optical applications such as phosphors and photocatalysts. Especially, unique photocatalysts can be designed by combining PMOs as a light collecting part and reaction sites placed in the mesochannels.

This paper reports on the construction of two types of novel PMO-based photocatalysts; (i) light harvesting[7] and (ii) electron donor-acceptor[8] photocatalysis systems.

2. Light Harvesting Photocatalysis System

2. 1 Preparation

A rhenium (Re) bipyridine complex was chosen as a reaction center because it is well-known two-electron-reduction photocatalysis of CO_2 to CO.[9] Bp-PMO was used as a light-harvesting antenna because of its well-studied optical properties and good spectral overlap of its emission band with the absorption band of the Re bipyridine complex for efficient FRET. The Re complex-immobilized Bp-PMO (Re/Bp-PMO) powder was prepared by two step processes as shown in **Fig. 2**. In the first step, Bp-PMO anchoring bipyridine (BPy) ligands on the walls of the mesochannels with Si-O-Si covalent bonds (BPy-Bp-PMO) was obtained by co-condensation of two-organosilane precursors, 1,4-bis(triethoxysilyl)biphenyl (BTEBP) and 4-[4-{3-(Trimethoxysilyl)propylsulfanyl}butyl]-4'-methyl-2,2'-bipyridine (SiBPy), in the presence of an octadecyltrimethylammonium chloride (C_{18}TMACl) surfactant under a basic condition. In this route, BPy can be homogeneously dispersed, especially in the mesochannels because the bipyridine unit and the attached alkyl chain are hydrophobic in nature and tend to enter into a core of the rod like surfactant micelles during the co-condensation process, which can promote homogeneous fixation of the Re complex in the mesochannels. The Re complex, *fac*-$[Re(BPy)(CO)_3(PPh_3)]^+(OTf)^-$ (BPy = the bipyridine unit anchored on the walls of the mesochannels) was formed by subsequent coordination of $[Re(CO)_5(PPh_3)]^+(OTf)^-$ to the bipyridine unit in BPy-Bp-PMO by refluxing in a toluene suspension.

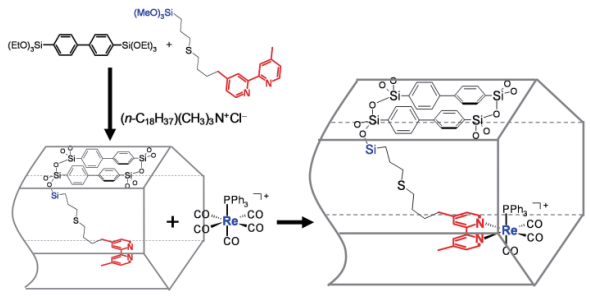

Fig. 2 A schematic image of the two-step synthesis of the rhenium(I) bipyridine complex ($[Re(BPy)(CO)_3(PPh_3)]^+$) fixed in Bp-PMO.

2. 2 Structural and Optical Properties

The x-ray diffraction (XRD) patterns of Re/Bp-PMO and BPy-Bp-PMO showed the existence of ordered mesochannels along with lamellar periodicity of the organic bridges in the pore walls, which indicates the preservation of the meso- and molecular-scale ordered structures of Bp-PMO during the co-condensation and post-coordination processes. The preservation was also confirmed by transmission electron microscopy. The nitrogen adsorption/desorption isotherms revealed that Re/Bp-PMO had large pore-volume (0.21 $cm^3\ g^{-1}$), specific surface area (520 $m^2\ g^{-1}$) and pore-diameter (2.9 nm), sufficient for mass transfer and catalytic reactions. The pore-volume of Re/Bp-PMO was smaller than those of Bp-PMO (0.49 $cm^3\ g^{-1}$) and BPy-Bp-PMO(0.33 $cm^3\ g^{-1}$) without any change in d-value (4.7 nm), which indicates that the Re complexes were mostly located within the mesochannels, because the decrease in pore-volume agreed well with the volume estimated from the molecular volume ($[Re(BPy)(CO)_3(PPh_3)](OTf)$, 0.859 nm^3) and the number of the Re complex introduced in Bp-PMO. The elemental analysis showed that the content of the Re complex in Re/Bp-PMO was 0.43 mmol g^{-1}, which corresponds to a Re/Bp molar ratio of 0.11 (Bp in Bp-PMO was 3.77 mmol g^{-1}).

The UV-vis diffuse reflectance spectrum of Re/Bp-PMO (**Fig. 3**: red) shows a metal-to-ligand charge transfer (MLCT) absorption band (λ_{max} = 345 nm) which corresponds to that of *fac*-$[Re(dmb)(CO)_3(PPh_3)]^+$ (dmb = 4,4'-dimethyl-2,2'-bipyridine) in CH_3CN (λ_{max} = 340 nm). The ν(C≡O) peaks at 2040, 1950, and 1930 cm^{-1} in the Fourier transform infrared (FT-IR) spectrum of Re/Bp-PMO indicate *fac*-$Re(CO)_3$ symmetry, in agreement with those of *fac*-$[Re(dmb)(CO)_3(PPh_3)]^+$ (2037, 1948, and 1925 cm^{-1} in CH_3CN). On the other hand, while Bp-PMO showed a strong fluorescence emission (λ_{max} = 380 nm, Φ =

0.42 ± 0.02, excited at 260 nm) from Bp in the framework (Fig. 3: black), Re/Bp-PMO showed almost no emission from Bp but exhibited a new emission band at 450-700 nm (excited at 260 nm) due to the Re complex (Fig. 3: blue). The results suggest that the excitation energy of Bp is completely transferred into the Re complex despite the low Re/Bp molar ratio. Although the Re complexes also absorb the excitation light (260 nm), their contribution is estimated to be quite low (ca. 5%), with consideration of the molar extinction coefficients (ε) in CH_3CN (ε = 27200 and 11700 $M^{-1}cm^{-1}$ for the organosilane precursor (BTEBP) and *fac*-$[Re(dmb)(CO)_3(PPh_3)]^+$, respectively, at 260 nm) and the molar ratio of Re/Bp (0.11). The measurement of the Re/Bp-PMO excited state lifetime also indicated dynamic quenching of the Bp excited state in the presence of the Re complex. Thus, the light-energy captured on the Bp-PMO antenna was efficiently funneled into the Re complex mainly by the FRET mechanism.

2. 3 Photocatalysis of CO_2 Reduction

The photocatalysis of CO_2 reduction was evaluated for Re/Bp-PMO (10 mg) dispersed in a mixture of an organic solvent (CH_3CN) and a sacrificial agent (triethanolamine; TEOA) (5:1 v/v, 50 mL). Monochromic light irradiation at 280 nm (excitation of Bp) under a CO_2 atmosphere generated CO (**Fig. 4**: red solid circles). For the initial 5 h, CO was constantly evolved with an apparent quantum yield (Φ_{CO}^{app}) of 1.2%, as estimated from the linear CO evolution rate and the light intensity (1.7×10^{-8} einstein s^{-1}). The total CO production for 24 h reached 6.2 μmol, which corresponds to a turnover number (TN_{CO}) of 2.2 based on the amount of Re atoms (2.9 μmol) in the slurry. The $^{13}CO_2$ (> 99 atom% enriched) tracer experiment produced 5.6 μmol of CO (over 24 h) consisting of ^{13}CO (68%) and ^{12}CO (32%). The presence of ^{12}CO can be reasonably explained by the ligand exchange from ^{12}CO to ^{13}CO in the photocatalytic cycle,[9] which was confirmed by FT-IR spectroscopy of the recovered sample. On the other hand, the tricarbonyl structure ($[Re(BPy)(CO)_3L]^+$, L = PPh_3 or $OCHO^-$) was completely preserved for Re/Bp-PMO without CO dissociation during the photoreaction, which was also confirmed by the FT-IR measurement. No CO was detected for Bp-PMO without the Re complex under photoirradiation at 280 nm, which indicates that the evolved CO does not originate from the organic component (Bp) of Bp-PMO (Fig. 4: black solid squares). These results clearly show the photocatalytic formation of CO from CO_2 by Re/Bp-PMO.

Photoirradiation to Re/Bp-PMO at 365 nm (direct excitation of the Re complex) with the same light intensity (1.7×10^{-8} einstein s^{-1}) resulted in a smaller amount of CO evolution (1.4 μmol for 24 h) (Fig. 4:

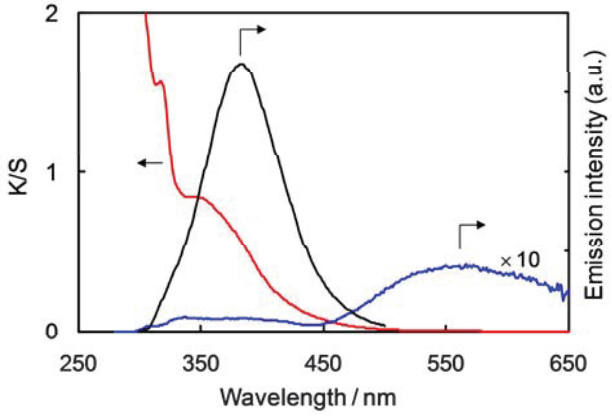

Fig. 3 UV-Vis diffuse reflectance spectrum of Re/Bp-PMO (red line) and emission spectra of Bp-PMO (black) and Re/Bp-PMO (blue) excited at 260 nm.

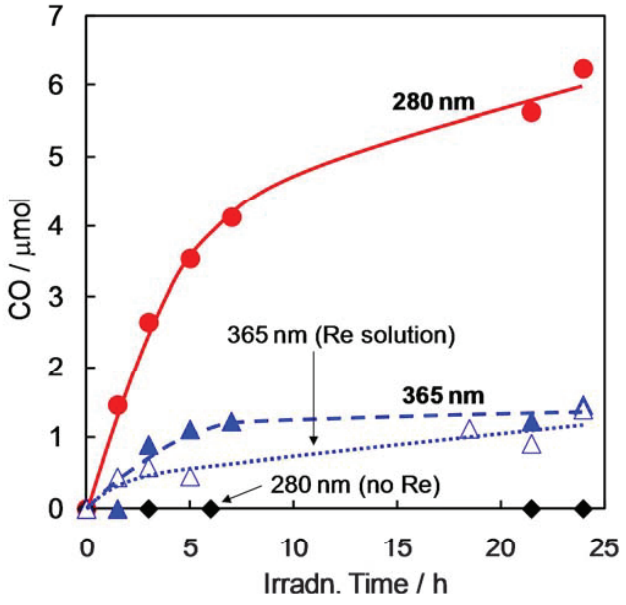

Fig. 4 CO generation by photocatalysis for CO_2 reduction on Re/Bp-PMO (Re: 3 μmol) under photoirradiation at 280 (●) and 365 nm (▲), and in a homogeneous $[Re(dmb)(CO)_3(PPh_3)]^+$ solution (0.06 mM; Re: 3 μmol) under photoirradiation at 365 nm (△). No CO generation was observed for Bp-PMO without the Re complex under photoirradiation at 280 nm (◆).

blue solid triangles). A homogeneous solution of *fac*-$[Re(dmb)(CO)_3(PPh_3)]^+$ also evolved a small amount of CO (1.4 μmol for 24 h at 365 nm) in CH_3CN/TEOA (5:1 v/v, 50 mL) with the same amount of the Re complex (3 μmol, 0.06 mM) in the reaction vessel as that in Re/Bp-PMO (Fig. 4: blue open triangles). Comparison of the amounts of CO evolved from Re/Bp-PMO under irradiation at 280 and 365 nm for 24 h indicates that the excitation of Bp sensitized the photocatalysis of the Re complex by a factor of 4.4. This result clearly shows the antenna effect of Bp-PMO for enhancing the photocatalysis of the Re complex (**Fig. 5**).

The Bp-PMO antenna showed an additional advantage in the stabilization of the Re complex in the mesochannels against UV light. Almost no decomposition of the Re complexes occurred for Re/Bp-PMO against irradiation at 280 nm, although the irradiation to *fac*-$[Re(dmb)(CO)_3(PPh_3)]^+$ molecules in a solution state resulted in dissociation of the CO ligands due to the formation of vibrationally hot states of the Re complexes by absorption of high-energy UV light ($\lambda < 313$ nm).[10] This can be explained by the mechanism that the Re complexes in Bp-PMO do not form higher excited states such as, $^1\pi$–π^* due to the absorption of high-energy photons by the Bp-PMO antenna, followed by relaxation to the lowest excited or excimer states of Bp.

3. Donor-acceptor Photocatalysis System

3. 1 Preparation

Bp-PMO was also chosen as the framework because of its well-defined mesoporous structure and well-studied optical properties. Viologen (Vio) was applied as an electron acceptor. The Vio groups were covalently attached onto the pore walls of Bp-PMO powder by a reaction of a Vio-bridged alkoxysilane, N,N'-bis(3-(trimethoxysilanyl)propyl)-4,4'-bipyridinium dihexafluorophosphate, with silanol groups of Bp-PMO in CH_3CN at 70°C for 2 h. The elemental analysis of nitrogen showed that the Vio-attached Bp-PMO (Vio-Bp-PMO) contained 33 μmol/g of Vio, corresponding to a molar Vio/Bp ratio of 1/118.

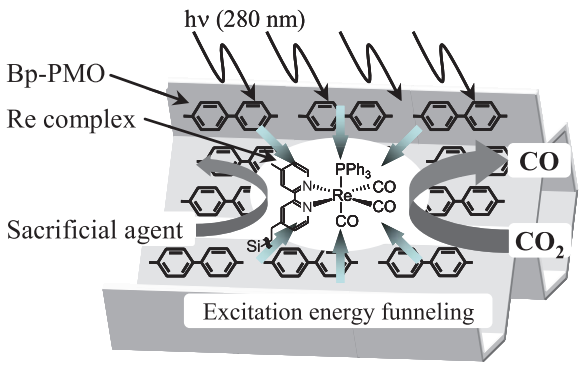

Fig. 5 A presumed scheme of the photocatalysis for Re/Bp-PMO.

3. 2 Structural and Optial Properties

The XRD pattern of Vio-Bp-PMO showed the existence of ordered mesochannels along with lamellar periodicity of the organic bridges in the pore walls, which indicates the preservation of the meso- and molecular-scale ordered structures of Bp-PMO after modification with Vio. The nitrogen adsorption/desorption isotherms of Vio-Bp-PMO showed the type-IV isotherm typical for mesoporous materials. Compared with Bp-PMO, the specific surface area and pore volume of Vio-Bp-PMO were reduced slightly from 842 to 796 m^2/g and from 0.51 to 0.44 cc/g, respectively, by modification with Vio, corresponding to successful attaching of Vio inside the mesochannels of Bp-PMO.

Figure 6 shows absorption spectra for the Bp and Vio precursors (0.05 mM in acetonitrile) and diffuse reflectance spectra for Bp-PMO and the Vio-Bp-PMO powders. The Bp and Vio precursors exhibited an absorption band at 263 and 264 nm respectively, while Bp-PMO displays a strong absorption with an edge at 320 nm. The absorbance recorded for Bp-PMO is saturated due to the dense packing of the absorptive Bp groups in the framework. The spectrum for Vio-Bp-PMO is largely similar to that of Bp-PMO except for an additional broad absorption band at 320–500 nm (Fig. 6, inset). Such an absorption band is typically observed for charge transfer (CT) complexes of viologen and aromatic donors, which suggests that the present material bears CT complexes formed between the attached Vio and Bp in the framework.

Figure 7 shows transient absorption spectra for Vio-Bp-PMO and the corresponding decay profiles in response to excitation of the CT band (355 nm). The spectra displayed a sharp absorption band at ca. 400 nm and broad absorption bands at ca. 600 and 720 nm. The band at 600 nm can be assignable to the Vio radical cations ($Vio^{\bullet+}$). The band at 720 nm is assigned to the Bp radical cations ($Bp^{\bullet+}$) from the transient absorption

spectrum measurement of the Bp precursor, exhibiting characteristic bands at 400 and 730 nm with a shoulder at 660 nm, in oxygen-saturated 2-propanol by biphotonic photoionization with a high powder laser. These bands are found to show red-shifts from those of radical cations of biphenyl molecules (390 and 680 nm with a shoulder at 630 nm) due to expansion of the π-conjugated length by silylation. The sharp band at 400 nm are attributed to both $Vio^{\bullet+}$ and $Bp^{\bullet+}$. These results indicate photo-induced electron transfer from Bp to Vio. The characteristic absorption bands of $Vio^{\bullet+}$ (600 nm) and $Bp^{\bullet+}$ (720 nm) decayed slowly with maintaining the spectral shape and both the radical cations showed almost the same decay profiles (Figs. 7(b) and 7(c)), suggestive of charge recombination between $Vio^{\bullet+}$ and $Bp^{\bullet+}$. The half-decay period of charge separation state was calculated to be approximately 10 μs, with more than 20% of the radical cations persisting even after 1 ms. This half-decay period is far longer than the nanosecond-scale decays estimated for CT crystals of viologen and aromatic donors based on first-order decay rate constants. Although the mechanism of persistent charge separation in Vio-Bp-PMO remains unclear, it is likely to be attributable to the stabilization of $Bp^{\bullet+}$ in the densely packed Bp groups of the framework. The charge separation in Vio-Bp-PMO is also more long-lived than for other typical photocatalysts such as TiO_2 (half-period of electron-hole recombination, <1 μs). The state of charge separation in the present material may therefore be advantageous for photocatalysis.

3. 3 Photocatalysis of H_2 Evolution

Photocatalytic hydrogen evolution was tested for Vio-Bp-PMO, since $Vio^{\bullet+}$ is known to drive the reduction of water to hydrogen with platinum (Pt). To prepare the photocatalyst, Vio-Bp-PMO was loaded with nanoparticulate Pt by photo-induced reduction of a Pt^{II} salt, forming Pt/Vio-Bp-PMO. Successful loading of nanoparticulate Pt into the mesochannels of Vio-Bp-PMO was confirmed by backscattered electron and dark-field scanning transmission electron microscopy, although aggregates of Pt nanoparticles were also detected outside of the mesochannels, resulting in a limited contact of Pt with Vio. The x-ray absorption fine structure (XAFS) spectrum indicated that Pt^{II} salts were partially reduced to metallic Pt.

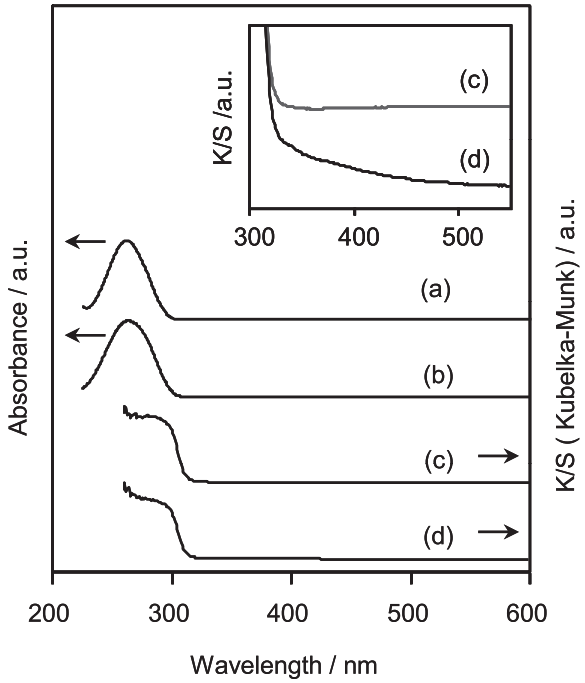

Fig. 6 Absorption spectra for the Bp (a) and Vio (b) precursors (0.05 mM in acetonitrile) and diffuse reflectance spectra for Bp-PMO (c) and Vio-Bp-PMO (d) powders. Vio-Bp-PMO displays a broad absorption band at 300–500 nm (inset).

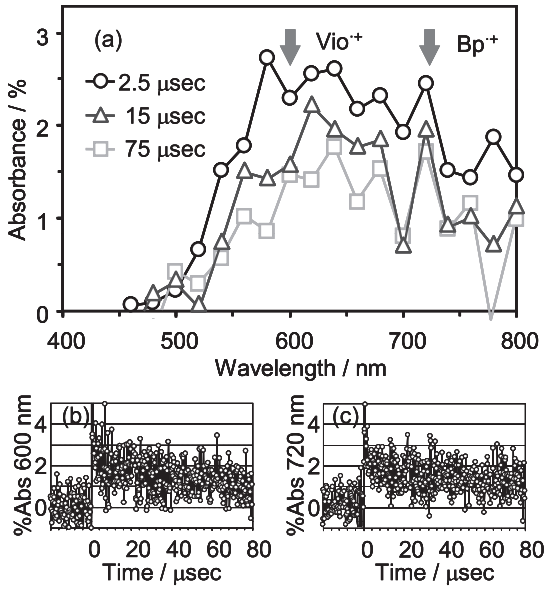

Fig. 7 (a) Transient absorption spectra for Vio-Bp-PMO upon excitation of the CT band at 355 nm. Absorption bands at ca. 600 and 720 nm correspond to $Vio^{\bullet+}$ and $Bp^{\bullet+}$, respectively. Decay profiles of the absorption at 600 nm ($Vio^{\bullet+}$) (b) and 720 nm ($Bp^{\bullet+}$) (c).

Hydrogen evolution using Pt/Vio-Bp-PMO in the presence of reduced nicotinamide adenine dinucleotide (NADH) as a sacrificial agent was performed under irradiation at 400 nm (**Fig. 8(**a)). Hydrogen was generated from water almost linearly with time after an induction period of 6–7 h. The reaction quantum yield after the induction period was 0.022%. In contrast, irradiation to a mixture of colloidal Pt and methylviologen (without Bp) at 400 nm did not result in hydrogen evolution, indicating that no photo-induced electron transfer occurs from NADH to methylviologen or Pt. Irradiation to Pt-loaded Bp-PMO (without Vio) at 400 nm resulted in very low hydrogen evolution (ca. 20% compared with that for Pt/Vio-Bp-PMO) associated with photo-induced electron transfer directly from Bp to Pt. In addition, a homogeneous solution system of Bp molecules, methylviologen and colloidal Pt also generated no hydrogen at the same photocatalysis conditions possibly due to a weaker electron-donating feature of molecular Bp than that of Bp in Bp-PMO, which suggests that the dense packing of Bp in the framework is effective for the electron donation. These results indicate that densely-packed Bp and Vio are essential for hydrogen evolution in this system, and that the reaction primarily proceeds by photo-induced charge separation between Bp and Vio, followed by electron transfer from Vio to Pt, consistent with the presumed mechanism (**Fig. 9**).

On the other hand, the low quantum yield of the present reaction (0. 022%) is likely to be due to the low density of the CT complexes on the surface of Bp-PMO (molar Vio/Bp ratio of 1/118) and/or the limited contact between Pt and Vio in the mesochannels, which reduces the contribution of electron transfer from Bp to Pt via Vio. In this process, significant increases in the Vio/Bp ratio and the Vio/Pt contact sites were difficult owing to the technical problems at now. To test whether an amount of the CT complex formation and/or Vio/Pt contact contribute significantly to photocatalytic activity, tests were carried out using Pt-loaded Bp-PMO in the presence of a large amount of free methylviologen (molar Vio/Bp ratio of 1/1). In this system, the free methylviologen is expected to act as an electron relay between the framework CT and Pt, enhancing the photocatalysis. In this reaction, hydrogen was evolved after induction period of 2 h at a reaction quantum yield of 0.39–0.56% (Fig. 8(b)). These results demonstrate that there remains further scope for improving the photocatalytic performance of this system.

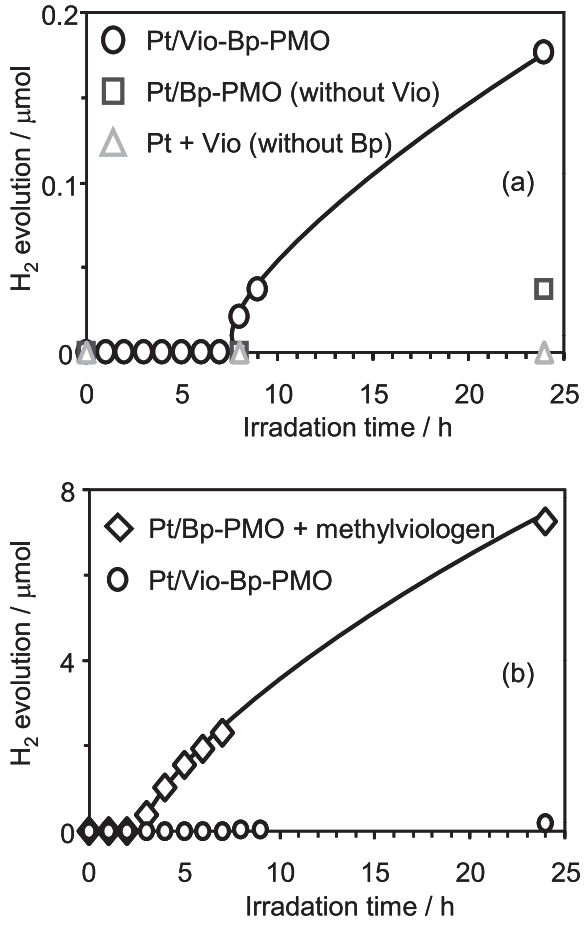

Fig. 8 (a) Hydrogen evolution from Pt/Vio-Bp-PMO and the reference systems in the presence of NADH under irradiation at 400 nm; Pt/Vio-Bp-PMO (○), Pt-PAA/methylviologen (without Bp: Δ) and Pt/Bp-PMO (without Vio: □). (b) Enhanced hydrogen evolution from Pt/Bp-PMO in the presence of large amounts of free methylviologen at the same photocatalysis conditions.

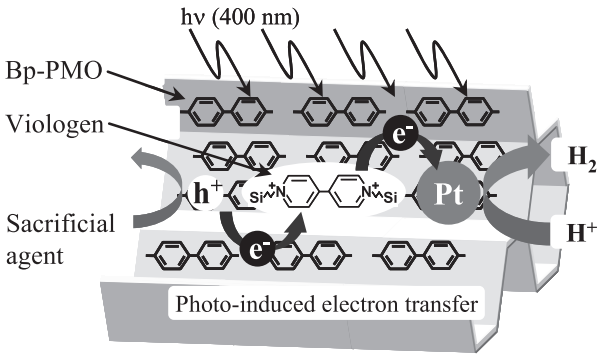

Fig. 9 A presumed scheme of the photocatalysis for Pt/Vio-Bp-PMO.

4. Conclusions

We constructed two types of novel photocatalysts utilizing light harvesting or photo-induced electron donating properties of Bp-PMO. For the light harvesting photocatalysis system, Re complexes were successfully fixed in the mesochannels of Bp-PMO by two step processes. For the obtained Re/Bp-PMO, light energy absorbed effectively by Bp in Bp-PMO was funneled into the Re complex in the mesochannels by FRET and sensitized photocatalytic CO evolution from CO_2 on the Re complex by a factor of 4.4 compared with direct excitation of the Re complex due to the light-harvesting of the PMO antenna. The PMO antenna also showed photoprotection effect on the CO-ligand dissociation from the Re complex by UV-light irradiation. For the donor-acceptor photocatalysis system, Vio was attached onto the pore walls of Bp-PMO, which resulted in the formation of CT complexes between the attached Vio and Bp in the framework. Excitation of the CT band was confirmed to induce electron transfer from Bp to Vio to promote persistent charge separation. Hydrogen was successfully evolved photocatalytically utilizing this charge separation mechanism for Pt-loaded Vio-Bp-PMO. These findings demonstrated the potential of PMO for construction of a broad spectrum of photocatalysts by appropriate combination of the organic groups in the framework (light collecting part) and catalysts (energy or electron accepting part).

Acknowledgments

Figures 2, 3 and 4 were reprinted with permission from the paper “Takeda, H., Ohashi, M., Tani, T., Ishitani, O. and Inagaki, S., *Inorg. Chem.*, Vol.49, No.10 (2010), p.4554-4559”. Copyright 2010, American Chemical Society. Figures 6, 7 and 8 were reprinted with permission from the paper “Ohashi, M., Aoki, M., Yamanaka, K., Nakajima, K., Ohsuna, T., Tani, T. and Inagaki, S., *Chem.-Eur. J.*, Vol.15, No.47 (2009), p.13041-13046”. Copyright 2009, John Wiley and Sons.

References

(1) (a) Loy, D. A. and Shea, K. J., *Chem. Rev.*, Vol.95, No.5 (1995), pp.1431-1442; (b) Shea, K. J., Loy, D. A. and Webster, O., *J. Am. Chem. Soc.*, Vol.114, No.17 (1992), pp.6700-6710; (c) Corriu, R. J. P., *Angew. Chem., Int. Ed.*, Vol.39, No.8 (2000), pp.1376-1398.

(2) (a) Inagaki, S., Guan, S., Fukushima, Y., Ohsuna, T. and Terasaki, O., *J. Am. Chem. Soc.*, Vol.121, No.41 (1999), pp.9611-9614; (b) Melde, B. J., Holland, B. T., Blanford, C. F. and Stein, A., *Chem. Mater.*, Vol.11, No.11 (1999), pp.3302-3308; (c) Asefa, T., MacLachlan, M. J., Coombs, N. and Ozin, G. A., *Nature*, Vol.402, No.6764 (1999), pp.867-871.

(3) (a) Hoffmann, F., Cornelius, M., Morell, J. and Fröba, M., *Angew. Chem., Int. Ed.*, Vol.45, No.20 (2006), pp.3216-3251; (b) Fujita, S. and Inagaki, S., *Chem. Mater.*, Vol.20, No.3 (2008), pp.891-908; (c) Yang, Q. H., Liu, J., Zhang, L. and Li, C., *J. Mater. Chem.*, Vol.19, No.14 (2009), pp.1945-1955; (d) Mizoshita, N., Tani, T. and Inagaki, S., *Chem. Soc. Rev.*, Vol.40, No.2 (2011), pp.789-800.

(4) (a) Inagaki, S., Guan, S., Ohsuna, T. and Terasaki, O., *Nature*, Vol.416, No.6878 (2002), pp.304-307; (b) Kapoor, M. P., Yang, Q. H. and Inagaki, S., *J. Am. Chem. Soc.*, Vol.124, No.51 (2002), pp.15176-15177; (c) Sayari, A. and Wang, W. H., *J. Am. Chem. Soc.*, Vol.127, No.35 (2005), pp.12194-12195; (d) Cornelius, M., Hoffmann, F. and Fröba, M., *Chem. Mater.*, Vol.17, No.26 (2005), pp.6674-6678; (e) Mizoshita, N., Goto, Y., Kapoor, M. P., Shimada, T., Tani, T. and Inagaki, S., *Chem.-Eur. J.*, Vol.15, No.1 (2009), pp.219-226.; (f) : Waki, M., Mizoshita, N., Ohsuna, T., , Tani, T. and Inagaki, S., *Chem. Commun.*, Vol.46, No.43 (2010), pp.8163-8165.

(5) Goto, Y., Mizoshita, N., Ohtani, O., Okada, T., Shimada, T., Tani, T. and Inagaki, S., *Chem. Mater.*, Vol.20, No.13 (2008), pp.4495-4498.

(6) Inagaki, S., Ohtani, O., Goto, Y., Okamoto, K., Ikai, M., Yamanaka, K., Tani, T. and Okada, T., *Angew. Chem., Int. Ed.*, Vol.48, No.22 (2009), pp.4042-4046.

(7) Takeda, H., Ohashi, M., Tani, T., Ishitani, O. and Inagaki, S., *Inorg. Chem.*, Vol.49, No.10 (2010), pp.4554-4559.

(8) Ohashi, M., Aoki, M., Yamanaka, K., Nakajima, K., Ohsuna, T., Tani, T. and Inagaki, S., *Chem.-Eur. J.*, Vol.15, No.47 (2009), pp.13041-13046.

(9) (a) Takeda, H., Koike, K., Inoue, H. and Ishitani, O., *J. Am. Chem. Soc.*, Vol.130, No.6 (2008), pp.2023-2031; (b) Takeda, H. and Ishitani, O., *Coord. Chem. Rev.*, Vol.254, No.3-4 (2010), pp.346-354.

(10) Sato, S., Sekine, A., Ohashi, Y., Ishitani, O., Blanco-Rodríguez, A. M., Vlček Jr., A., Unno, T. and Koike, K., *Inorg. Chem*., Vol.46, No.9 (2007), pp.3531-3540.

Takao Tani

Research Fields:
- Functionalization of Periodic Mesoporous Organosilicas
- Flame Synthesis of Metal Oxide Nanoparticles and Their Applications

Academic Degree: Dr. sc. techn. ETH
Academic Societies:
- The Ceramic Society of Japan
- The Japanese Sol-Gel Society

Awards:
- 40th Tokai Chemical Industry Association Award, 2005

Hiroyuki Takeda

Research Field:
- Photo-Functionalization, especially Construction of Photocatalysts Using Mesoporous Organosilicas and Metal Complexes

Academic Degree: Dr. Sci.
Academic Societies:
- The Chemical Society of Japan
- The Japanese Photochemistry Association

Award:
- 6th International Mesostructured Materials Symposium, Best Poster Presentation Awards, 2008

Masataka Ohashi

Research Field:
- Functionalization of Periodic Mesoporous Organosilicas

Academic Degree: Dr. Sci.
Academic Societies:
- The Chemical Society of Japan
- Catalysis Society of Japan

Shinji Inagaki

Research Field:
- Synthesis and Applications of Mesoporous Materials

Academic Degree: Dr. Eng.
Academic Societies:
- The Chemical Society of Japan
- Catalysis Society of Japan
- Japan Association of Zeolite
- The Japan Society on Adsorption
- The Society of Polymer Science, Japan
- International Mesostructured Materials Association
- International Zeolite Association

Awards:
- The Award of Chemistry on Catalyst Preparation, 1994
- The Promotion Award of the Japan Society on Adsorption, 2001
- The Chemical Society of Japan Award for Creative Work for 2004
- The Minister Award of Education, Culture, Sport, Science and Technology, 2005
- The Japan Society on Adsorption Award, 2008

